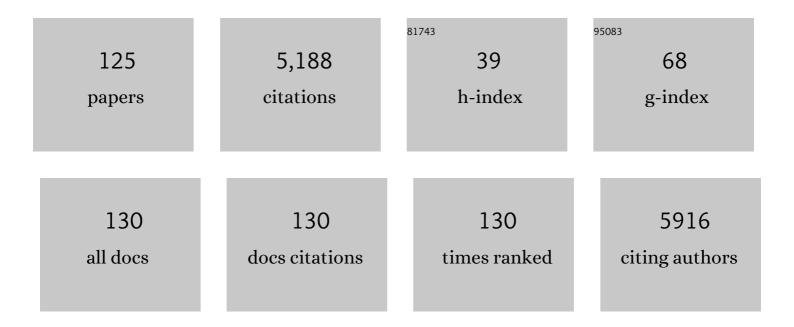
Boaz Pokroy

List of Publications by Year in descending order

Source: https://exaly.com/author-pdf/7410808/publications.pdf Version: 2024-02-01



#	Article	IF	CITATIONS
1	Self-Organization of a Mesoscale Bristle into Ordered, Hierarchical Helical Assemblies. Science, 2009, 323, 237-240.	6.0	368
2	Bacterial biofilm shows persistent resistance to liquid wetting and gas penetration. Proceedings of the United States of America, 2011, 108, 995-1000.	3.3	302
3	An artificial biomineral formed by incorporation of copolymer micelles in calcite crystals. Nature Materials, 2011, 10, 890-896.	13.3	248
4	Tuning hardness in calcite by incorporation of amino acids. Nature Materials, 2016, 15, 903-910.	13.3	183
5	Anisotropic lattice distortions in biogenic aragonite. Nature Materials, 2004, 3, 900-902.	13.3	175
6	Anisotropic lattice distortions in biogenic calcite induced by intra-crystalline organic molecules. Journal of Structural Biology, 2006, 155, 96-103.	1.3	171
7	Fabrication of Bioinspired Actuated Nanostructures with Arbitrary Geometry and Stiffness. Advanced Materials, 2009, 21, 463-469.	11.1	167
8	A hydrated crystalline calcium carbonate phase: Calcium carbonate hemihydrate. Science, 2019, 363, 396-400.	6.0	153
9	Vaterite Crystals Contain Two Interspersed Crystal Structures. Science, 2013, 340, 454-457.	6.0	139
10	Anisotropic lattice distortions in the mollusk-made aragonite: A widespread phenomenon. Journal of Structural Biology, 2006, 153, 145-150.	1.3	126
11	Screening the Incorporation of Amino Acids into an Inorganic Crystalline Host: the Case of Calcite. Advanced Functional Materials, 2012, 22, 4216-4224.	7.8	124
12	Biogenic Guanine Crystals from the Skin of Fish May Be Designed to Enhance Light Reflectance. Crystal Growth and Design, 2008, 8, 507-511.	1.4	118
13	The Microstructure of Biogenic Calcite: A View by High-Resolution Synchrotron Powder Diffraction. Advanced Materials, 2006, 18, 2363-2368.	11.1	117
14	Powder diffraction and crystal structure prediction identify four new coumarin polymorphs. Chemical Science, 2017, 8, 4926-4940.	3.7	97
15	Coherently aligned nanoparticles within a biogenic single crystal: A biological prestressing strategy. Science, 2017, 358, 1294-1298.	6.0	97
16	Atomic Structure of Biogenic Aragonite. Chemistry of Materials, 2007, 19, 3244-3251.	3.2	87
17	On the structure of aragonite. Acta Crystallographica Section B: Structural Science, 2005, 61, 129-132.	1.8	86
18	Bioâ€Inspired Band Gap Engineering of Zinc Oxide by Intracrystalline Incorporation of Amino Acids. Advanced Materials, 2014, 26, 477-481.	11.1	82

#	Article	IF	CITATIONS
19	"Guanigma― The Revised Structure of Biogenic Anhydrous Guanine. Chemistry of Materials, 2015, 27, 8289-8297.	3.2	74
20	Resorcinol Crystallization from the Melt: A New Ambient Phase and New "Riddles― Journal of the American Chemical Society, 2016, 138, 4881-4889.	6.6	74
21	Electrochemical behaviour of stainless steels in media containing iron-oxidizing bacteria (IOB) by corrosion process modeling. Corrosion Science, 2008, 50, 540-547.	3.0	71
22	Hierarchical Calcite Crystals with Occlusions of a Simple Polyelectrolyte Mimic Complex Biomineral Structures. Advanced Functional Materials, 2012, 22, 4668-4676.	7.8	69
23	Microstructure of natural plywood-like ceramics: a study by high-resolution electron microscopy and energy-variable X-ray diffraction. Journal of Materials Chemistry, 2003, 13, 682-688.	6.7	67
24	Control of Shape and Size of Nanopillar Assembly by Adhesion-Mediated Elastocapillary Interaction. ACS Nano, 2010, 4, 6323-6331.	7.3	63
25	Structure and Properties of Nanocomposites Formed by the Occlusion of Block Copolymer Worms and Vesicles Within Calcite Crystals. Advanced Functional Materials, 2016, 26, 1382-1392.	7.8	63
26	Oxygen Spectroscopy and Polarization-Dependent Imaging Contrast (PIC)-Mapping of Calcium Carbonate Minerals and Biominerals. Journal of Physical Chemistry B, 2014, 118, 8449-8457.	1.2	60
27	Intracrystalline inclusions within single crystalline hosts: from biomineralization to bio-inspired crystal growth. CrystEngComm, 2015, 17, 5873-5883.	1.3	59
28	Biomineralization of calcium carbonate: structural aspects. CrystEngComm, 2007, 9, 1156.	1.3	58
29	Sponge-associated bacteria mineralize arsenic and barium on intracellular vesicles. Nature Communications, 2017, 8, 14393.	5.8	55
30	Crystal nucleation and near-epitaxial growth in nacre. Journal of Structural Biology, 2013, 184, 454-463.	1.3	54
31	Structure of Biogenic Aragonite (CaCO ₃). Crystal Growth and Design, 2007, 7, 1580-1583.	1.4	52
32	Protein mapping of calcium carbonate biominerals by immunogold. Biomaterials, 2007, 28, 2368-2377.	5.7	49
33	Bioinspired passive anti-biofouling surfaces preventing biofilm formation. Journal of Materials Chemistry B, 2015, 3, 1371-1378.	2.9	49
34	Additives Control the Stability of Amorphous Calcium Carbonate via Two Different Mechanisms: Surface Adsorption versus Bulk Incorporation. Advanced Functional Materials, 2020, 30, 2000003.	7.8	49
35	Protein-induced, previously unidentified twin form of calcite. Proceedings of the National Academy of Sciences of the United States of America, 2007, 104, 7337-7341.	3.3	46
36	Incorporation of a Recombinant Biomineralization Fusion Protein into the Crystalline Lattice of Calcite. Chemistry of Materials, 2014, 26, 4925-4932.	3.2	45

#	Article	IF	CITATIONS
37	Calcite shape modulation through the lattice mismatch between the self-assembled monolayer template and the nucleated crystal face. CrystEngComm, 2007, 9, 1219.	1.3	40
38	Nacre in Mollusk Shells as a Multilayered Structure with Strain Gradient. Advanced Functional Materials, 2009, 19, 1054-1059.	7.8	40
39	Selfâ€Assembling, Bioinspired Wax Crystalline Surfaces with Timeâ€Dependent Wettability. Advanced Functional Materials, 2012, 22, 745-750.	7.8	40
40	Coiled to Diffuse: Brownian Motion of a Helical Bacterium. Langmuir, 2012, 28, 12941-12947.	1.6	39
41	Bioâ€Inspired Superoleophobic Fluorinated Wax Crystalline Surfaces. Advanced Functional Materials, 2013, 23, 4572-4576.	7.8	39
42	Purification and Functional Analysis of a 40 kD Protein Extracted from theStrombus decorus persicusMollusk Shells. Biomacromolecules, 2006, 7, 550-556.	2.6	37
43	From spinodal decomposition to alternating layered structure within single crystals of biogenic magnesium calcite. Nature Communications, 2019, 10, 4559.	5.8	36
44	Residual Strain and Stress in Biocrystals. Advanced Materials, 2018, 30, e1707263.	11.1	35
45	Size Effect on the Short Range Order and the Crystallization of Nanosized Amorphous Alumina. Crystal Growth and Design, 2014, 14, 3983-3989.	1.4	34
46	Calcite Single Crystals as Hosts for Atomicâ€ s cale Entrapment and Slow Release of Drugs. Advanced Healthcare Materials, 2015, 4, 1510-1516.	3.9	32
47	Exposed and Buried Biomineral Interfaces in the Aragonitic Shell of <i>Perna canaliculus</i> Revealed by Solid-State NMR. Chemistry of Materials, 2013, 25, 4595-4602.	3.2	31
48	Sponge-like nanoporous single crystals of gold. Nature Communications, 2015, 6, 8841.	5.8	31
49	Additives influence the phase behavior of calcium carbonate solution by a cooperative ion-association process. Journal of Materials Chemistry B, 2018, 6, 449-457.	2.9	31
50	Narrowly Distributed Crystal Orientation in Biomineral Vaterite. Chemistry of Materials, 2015, 27, 6516-6523.	3.2	27
51	Molecular and skeletal fingerprints of scleractinian coral biomineralization: From the sea surface to mesophotic depths. Acta Biomaterialia, 2021, 120, 263-276.	4.1	27
52	Sonication-Assisted Synthesis of Large, High-Quality Mercury Thiolate Single Crystals Directly from Liquid Mercury. Journal of the American Chemical Society, 2010, 132, 14355-14357.	6.6	26
53	Bio-inspired engineering of a zinc oxide/amino acid composite: synchrotron microstructure study. CrystEngComm, 2014, 16, 3268-3273.	1.3	25
54	Aragonite growth on single-crystal substrates displaying a threefold axis. Chemical Communications, 2005, , 2140.	2.2	24

#	Article	IF	CITATIONS
55	Biofabrication of Nanocellulose–Mycelium Hybrid Materials. Advanced Sustainable Systems, 2021, 5, 2000196.	2.7	24
56	Bioinspired hierarchical superhydrophobic structures formed by n-paraffin waxes of varying chain lengths. Soft Matter, 2013, 9, 5710.	1.2	23
57	Bioinspired Nanocomposites: Ordered 2D Materials Within a 3D Lattice. Advanced Functional Materials, 2016, 26, 5569-5575.	7.8	23
58	Multilevel Hierarchy of Fluorinated Wax on CuO Nanowires for Superoleophobic Surfaces. Langmuir, 2014, 30, 15568-15573.	1.6	21
59	Insect attachment on crystalline bioinspired wax surfaces formed by alkanes of varying chain lengths. Beilstein Journal of Nanotechnology, 2014, 5, 1031-1041.	1.5	20
60	Three-Dimensional Triple Hierarchy Formed by Self-Assembly of Wax Crystals on CuO Nanowires for Nonwettable Surfaces. ACS Applied Materials & amp; Interfaces, 2014, 6, 4927-4934.	4.0	20
61	Lattice Shrinkage by Incorporation of Recombinant Starmakerâ€Like Protein within Bioinspired Calcium Carbonate Crystals. Chemistry - A European Journal, 2019, 25, 12740-12750.	1.7	20
62	Shape of Water–Air Interface beneath a Drop on a Superhydrophobic Surface Revealed: Constant Curvature That Approaches Zero. Journal of Physical Chemistry C, 2013, 117, 6658-6663.	1.5	18
63	Structural analysis of metal-doped calcium oxalate. RSC Advances, 2015, 5, 98626-98633.	1.7	18
64	Photocatalytic activity of exfoliated graphite–TiO ₂ nanoparticle composites. Nanoscale, 2019, 11, 19301-19314.	2.8	18
65	A study on the wetting properties of broccoli leaf surfaces and their time dependent self-healing after mechanical damage. Soft Matter, 2018, 14, 7782-7792.	1.2	17
66	Acidic Monosaccharides become Incorporated into Calcite Single Crystals**. Chemistry - A European Journal, 2020, 26, 16860-16868.	1.7	17
67	Strong Band Gap Blueshift in Copper (I) Oxide Semiconductor via Bioinspired Route. Advanced Functional Materials, 2020, 30, 1910405.	7.8	17
68	Formation and Elimination of Surface Nanodefects on Ultraflat Metal Surfaces Produced by Template Stripping. Langmuir, 2011, 27, 13415-13419.	1.6	16
69	Unique crystallographic pattern in the macro to atomic structure of Herdmania momus vateritic spicules. Journal of Structural Biology, 2013, 183, 191-198.	1.3	16
70	Pore and ligament size control, thermal stability and mechanical properties of nanoporous single crystals of gold. Nanoscale, 2017, 9, 14458-14466.	2.8	16
71	Crystallization of Malonic and Succinic Acids on SAMs: Toward the General Mechanism of Oriented Nucleation on Organic Monolayers. Langmuir, 2009, 25, 14002-14006.	1.6	15
72	Atomic structure and ultrastructure of the Murex troscheli shell. Journal of Structural Biology, 2012, 180, 539-545.	1.3	15

#	Article	IF	CITATIONS
73	Hybrid Gold Single Crystals Incorporating Amino Acids. Crystal Growth and Design, 2016, 16, 2972-2978.	1.4	14
74	Effect of Surface Chemistry on Incorporation of Nanoparticles within Calcite Single Crystals. Crystal Growth and Design, 2019, 19, 4429-4435.	1.4	14
75	Thickness dependence of the physical properties of atomic-layer deposited Al2O3. Journal of Applied Physics, 2019, 125, .	1.1	14
76	High Amino Acid Lattice Loading at Nonambient Conditions Causes Changes in Structure and Expansion Coefficient of Calcite. Chemistry of Materials, 2020, 32, 4205-4212.	3.2	14
77	Strong Quantum Confinement Effects and Chiral Excitons in Bio-Inspired ZnO–Amino Acid Cocrystals. Journal of Physical Chemistry C, 2018, 122, 6348-6356.	1.5	13
78	Superhydrophobic Wax Coatings for Prevention of Biofilm Establishment in Dairy Food. ACS Applied Bio Materials, 2019, 2, 4932-4940.	2.3	13
79	Selfâ€Propulsion of Droplets via Lightâ€Stimuli Rapid Control of Their Surface Tension. Advanced Materials Interfaces, 2021, 8, 2100751.	1.9	13
80	A comparison between HfO2/Al2O3 nano-laminates and ternary HfxAlyO compound as the dielectric material in InGaAs based metal-oxide-semiconductor (MOS) capacitors. Journal of Applied Physics, 2016, 120, 124505.	1.1	12
81	Synthesis of calcium carbonate in trace water environments. Chemical Communications, 2017, 53, 4811-4814.	2.2	12
82	Incorporation of organic and inorganic impurities into the lattice of metastable vaterite. Inorganic Chemistry Frontiers, 2019, 6, 2696-2703.	3.0	12
83	Structure and Morphology of Light-Reflecting Synthetic and Biogenic Polymorphs of Isoxanthopterin: A Comparison. Chemistry of Materials, 2019, 31, 4479-4489.	3.2	12
84	Retinoic acid/calcite micro-carriers inserted in fibrin scaffolds modulate neuronal cell differentiation. Journal of Materials Chemistry B, 2019, 7, 5808-5813.	2.9	11
85	Helical Microstructures of the Mineralized Coralline Red Algae Determine Their Mechanical Properties. Advanced Science, 2020, 7, 2000108.	5.6	11
86	Density of Nanometrically Thin Amorphous Films Varies by Thickness. Chemistry of Materials, 2017, 29, 4912-4919.	3.2	10
87	A fungal mycelium templates the growth of aragonite needles. Journal of Materials Chemistry B, 2019, 7, 5725-5731.	2.9	10
88	Bioinspired Molecular Bridging in a Hybrid Perovskite Leads to Enhanced Stability and Tunable Properties. Advanced Functional Materials, 2020, 30, 2005136.	7.8	10
89	Coral micro- and macro-morphological skeletal properties in response to life-long acclimatization at CO2 vents in Papua New Guinea. Scientific Reports, 2021, 11, 19927.	1.6	10
90	High-Mg calcite nanoparticles within a low-Mg calcite matrix: A widespread phenomenon in biomineralization. Proceedings of the National Academy of Sciences of the United States of America, 2022, 119, e2120177119.	3.3	10

#	Article	IF	CITATIONS
91	Long-term stabilized amorphous calcium carbonate—an ink for bio-inspired 3D printing. Materials Today Bio, 2021, 11, 100120.	2.6	9
92	Depth-resolved strain measurements in polycrystalline materials by energy-variable X-ray diffraction. Journal of Synchrotron Radiation, 2004, 11, 309-313.	1.0	8
93	Structural analysis and optical properties of the Bi _{2â^'x} Y _x WO ₆ system. CrystEngComm, 2016, 18, 6464-6470.	1.3	8
94	Non-stoichiometric hydrated magnesium-doped calcium carbonate precipitation in ethanol. Chemical Communications, 2019, 55, 12944-12947.	2.2	8
95	Inhomogeneous Strain/Stress Profiles in the Nacre Layer of Mollusk Shells. Metallurgical and Materials Transactions A: Physical Metallurgy and Materials Science, 2011, 42, 554-558.	1.1	7
96	Insights on the interaction of calcein with calcium carbonate and its implications in biomineralization studies. CrystEngComm, 2018, 20, 4221-4224.	1.3	7
97	Formation of Curved Micrometer-Sized Single Crystals. ACS Nano, 2014, 8, 4747-4753.	7.3	6
98	Morphology-preserving transformation of minerals mediated by a temperature-responsive polymer membrane: calcite to hydroxyapatite. CrystEngComm, 2016, 18, 2289-2293.	1.3	6
99	Morphological changes of calcite single crystals induced by graphene–biomolecule adducts. Journal of Crystal Growth, 2017, 457, 356-361.	0.7	6
100	Experimental and Theoretical Insights into the Bioinspired Formation of Disordered Ba alcite. Advanced Functional Materials, 2020, 30, 1805028.	7.8	6
101	Structural and chemical variations in Mg-calcite skeletal segments of coralline red algae lead to improved crack resistance. Acta Biomaterialia, 2021, 130, 362-373.	4.1	6
102	Adsorption of SARS CoV-2 spike proteins on various functionalized surfaces correlates with the high transmissibility of Delta and Omicron variants. Materials Today Bio, 2022, 14, 100265.	2.6	6
103	Amorphous biogenic calcium oxalate. ChemistrySelect, 2016, 1, 132-135.	0.7	5
104	Kinetics of Nanoscale Self-Assembly Measured on Liquid Drops by Macroscopic Optical Tensiometry: From Mercury to Water and Fluorocarbons. Journal of the American Chemical Society, 2016, 138, 2585-2591.	6.6	5
105	Tuning the Magnetization of Manganese (II) Carbonate by Intracrystalline Amino Acids. Advanced Materials, 2022, 34, .	11.1	5
106	Paraffin Wax Crystal Coarsening: Effects of Strain and Wax Crystal Shape. Crystal Growth and Design, 2016, 16, 3932-3939.	1.4	4
107	Association Between Gold Grain Orientation and Its Periodic Steps Formed at the Gold/Substrate Interface. Journal of Physical Chemistry C, 2018, 122, 11364-11370.	1.5	4
108	Surface reconstruction causes structural variations in nanometric amorphous Al ₂ O ₃ . Physical Chemistry Chemical Physics, 2019, 21, 14887-14891.	1.3	4

#	Article	IF	CITATIONS
109	Retention of surface structure causes lower density in atomic layer deposition of amorphous titanium oxide thin films. Physical Chemistry Chemical Physics, 2021, 23, 6600-6612.	1.3	4
110	On the mechanism of calcium carbonate polymorph selection <i>via</i> confinement. Faraday Discussions, 2022, 235, 433-445.	1.6	4
111	Disorder and Confinement Effects to Tune the Optical Properties of Amino Acid Doped Cu ₂ O Crystals. Advanced Functional Materials, 2022, 32, .	7.8	4
112	Self-Ordered Vicinal-Surface-Like Nanosteps at the Thin Metal-Film/Substrate Interface. Journal of Physical Chemistry C, 2012, 116, 12149-12155.	1.5	3
113	Selective Deposition of Platinum by Atomic Layer Deposition Using Terraced Oxide Surfaces. Journal of Physical Chemistry C, 2019, 123, 8770-8776.	1.5	3
114	Modifying hydrophilic properties of polyurethane acryl paint substrates by atomic layer deposition and self-assembled monolayers. RSC Advances, 2020, 10, 34333-34343.	1.7	3
115	Excessive Increase in the Optical Band Gap of Nearâ€Infrared Semiconductor Lead (II) Sulfide via the Incorporation of Amino Acids. Advanced Optical Materials, 0, , 2200203.	3.6	3
116	Measurement of Residual Strains with High Depth Resolution by Energy-Variable Diffraction on Synchrotron Beam Lines. Materials Research Society Symposia Proceedings, 2004, 840, Q7.7.1.	0.1	2
117	A Gold Complex Single Crystal Comprising Nanoporosity and Curved Surfaces. Crystal Growth and Design, 2017, 17, 221-227.	1.4	2
118	Climate variation during the Holocene influenced the skeletal properties of Chamelea gallina shells in the North Adriatic Sea (Italy). PLoS ONE, 2021, 16, e0247590.	1.1	2
119	Self-catalytic growth of one-dimensional materials within dislocations in gold. Proceedings of the National Academy of Sciences of the United States of America, 2021, 118, .	3.3	2
120	Superhydrophobic Surfaces: Selfâ€Assembling, Bioinspired Wax Crystalline Surfaces with Timeâ€Dependent Wettability (Adv. Funct. Mater. 4/2012). Advanced Functional Materials, 2012, 22, 744-744.	7.8	1
121	Semiconductors: Bio-Inspired Band Cap Engineering of Zinc Oxide by Intracrystalline Incorporation of Amino Acids (Adv. Mater. 3/2014). Advanced Materials, 2014, 26, 503-503.	11.1	1
122	Sclerites of the soft coral Ovabunda macrospiculata (Xeniidae) are predominantly the metastable CaCO3 polymorph vaterite. Acta Biomaterialia, 2021, 135, 663-670.	4.1	1
123	Structural Distinctions Between Biogenic and Geological Aragonite. Materials Research Society Symposia Proceedings, 2005, 874, 1.	0.1	0
124	Superoleophobic Materials: Bio-Inspired Superoleophobic Fluorinated Wax Crystalline Surfaces (Adv.) Tj ETQq0 0	0 _{7g} BT /O	verlock 10 Tf

125	Lattice Shrinkage by Incorporation of Recombinant Starmakerâ€Like Protein within Bioinspired Calcium Carbonate Crystals. Chemistry - A European Journal, 2019, 25, 12658-12658.	1.7	0	
-----	--	-----	---	--